# Soluble and Membrane-Bound β-Glucosidases Are Involved in Trimming the Xyloglucan Backbone[1][OPEN]

**Javier Sampedro, Elene R. Valdivia, Patricia Fraga, Natalia Iglesias, Gloria Revilla, and Ignacio Zarra***

Departemento Biología Funcional, Facultad de Biología, Universidad de Santiago, Santiago de Compostela, 15782 Spain

**ORCID IDs: 0000-0002-6534-5347 (J.S.); 0000-0001-6773-0583 (E.R.V.); 0000-0001-9053-4134 (N.I.); 0000-0002-2150-8538 (G.R.); 0000-0001-7203-0688 (I.Z.).**

In many flowering plants, xyloglucan is a major component of primary cell walls, where it plays an important role in growth regulation. Xyloglucan can be degraded by a suite of exoglycosidases that remove specific sugars. In this work, we show that the xyloglucan backbone, formed by (1→4)-linked β-D-glucopyranosyl residues, can be attacked by two different Arabidopsis (*Arabidopsis thaliana*) β-glucosidases from glycoside hydrolase family 3. While BGLC1 (At5g20950; for β-glucosidase active against xyloglucan 1) is responsible for all or most of the soluble activity, BGLC3 (At5g04885) is usually a membrane-anchored protein. Mutations in these two genes, whether on their own or combined with mutations in other exoglycosidase genes, resulted in the accumulation of partially digested xyloglucan subunits, such as GXXG, GXLG, or GXFG. While a mutation in *BGLC1* had significant effects on its own, lack of *BGLC3* had only minor effects. On the other hand, double *bglc1 bglc3* mutants revealed a synergistic interaction that supports a role for membrane-bound BGLC3 in xyloglucan metabolism. In addition, *bglc1 bglc3* was complemented by overexpression of either *BGLC1* or *BGLC3*. In overexpression lines, BGLC3 activity was concentrated in a microsome-enriched fraction but also was present in soluble form. Finally, both genes were generally expressed in the same cell types, although, in some cases, *BGLC3* was expressed at earlier stages than *BGLC1*. We propose that functional specialization could explain the separate localization of both enzymes, as a membrane-bound β-glucosidase could specifically digest soluble xyloglucan without affecting the wall-bound polymer.

Plant cell growth is regulated by the interaction between turgor pressure and the mechanical properties of the primary cell wall (Wolf et al., 2012). This wall is a composite of rigid and stable cellulose microfibrils embedded in a matrix of more flexible and metabolically active polysaccharides. In Arabidopsis (*Arabidopsis thaliana*), as in most angiosperms, xyloglucan and pectins form the bulk of this matrix.

All xyloglucans have a backbone of (1→4)-linked β-D-glucopyranosyl residues, a large proportion of which are substituted with side chains (Schultink et al., 2014). In the standard nomenclature, G represents unsubstituted Glc while X indicates Glc residues substituted with α-D-xylopyranosyl at O6 (Fry et al., 1993; Tuomivaara et al., 2015). An additional β-D-galactopyranosyl attached at the O2 of the xylose is denoted by L, and an F is used when this Gal is further substituted with α-L-fucopyranosyl at O2. These are the most common side chains in Arabidopsis, but other types have been described in different species or specialized cell types, such as root hairs (Peña et al., 2012; Schultink et al., 2014). Arabidopsis xyloglucan belongs to the XXXG type, which typically has one unsubstituted Glc every four residues. Treatment of Arabidopsis xyloglucan with endoglucanases that attack these Glc residues results in oligosaccharide mixtures dominated by XXXG, XXLG, XXFG, and XLFG subunits (Lerouxel et al., 2002; Vanzin et al., 2002). Many of the Gal residues in Arabidopsis xyloglucan are *O*-acetylated, and this is indicated by underlining the side chain symbol, as in XLFG (Schultink et al., 2014).

Xyloglucans are synthesized in the Golgi apparatus by a suite of enzymes and transported to the wall in secretory vesicles (Pauly and Keegstra, 2016). What happens to this polymer after being released and how it becomes integrated into the cell wall network are not fully understood (Park and Cosgrove, 2015). A certain amount of xyloglucan appears to be trapped inside microfibrils, which could happen during the crystallization process (Pauly et al., 1999; Dick-Pérez et al., 2011). It is also well known that xyloglucan can bind to the surface of cellulose (Hayashi, 1989), but NMR studies suggest that, in vivo, only a small portion of microfibril surfaces are coated with this polymer, possibly due to competition with pectins (Bootten et al., 2004; Dick-Pérez et al., 2011). Thus, a large portion of

[1] This work was supported by the Ministerio de Economía y Competividad (grant no. BIO2012-40032-C03-01) and the Xunta de Galicia (grant no. PGIDIT10PXIB200305PR), Spain.

* Address correspondence to ignacio.zarra@usc.es.

The author responsible for distribution of materials integral to the findings presented in this article in accordance with the policy described in the Instructions for Authors (www.plantphysiol.org) is: Ignacio Zarra (ignacio.zarra@usc.es).

J.S. designed and performed experiments, analyzed the data, and wrote the article; E.R.V., P.F., and N.I. performed experiments; G.R. and I.Z. supervised experiments and participated in writing the article.

[OPEN] Articles can be viewed without a subscription.

www.plantphysiol.org/cgi/doi/10.1104/pp.16.01713

  

xyloglucan could be present in the space between microfibrils in a more or less relaxed conformation, where it would be accessible to different enzymes.

Xyloglucan has an important role in the regulation of cell wall extension. Arabidopsis mutants with no detectable xyloglucan are significantly smaller, and they show altered guard cell dynamics, irregularly spaced microfibrils, and reduced wall extension in response to low pH or α-expansins (Park and Cosgrove, 2012a; Rui and Anderson, 2016; Xiao et al., 2016). Exogenous xyloglucan application also can reduce wall extension (Takeda et al., 2002). In addition, wall extension can be induced directly by endoglucanases capable of digesting both cellulose and xyloglucan but not by those that only attack one or the other (Park and Cosgrove, 2012b). A recent proposal is that xyloglucan chains are an integral part of load-bearing complexes that are formed where neighboring microfibrils come in close contact (Park and Cosgrove, 2015).

Different activities participate in xyloglucan metabolism in the wall. Xyloglucan chains can be cut by xyloglucan transglycosylases/hydrolases (XTHs) on the reducing end side of unsubstituted Glc residues (Eklöf and Brumer, 2010). Most enzymes in this family show predominantly xyloglucan endotransglucosylase activity, reattaching newly created reducing ends to the nonreducing end of another molecule. These activities could modify xyloglucan chain length as well as its connections to microfibrils and have been shown to alter cell wall extension (Nishitani and Vissenberg, 2007; Miedes et al., 2013; Park and Cosgrove, 2015). The family also includes enzymes that show predominantly endohydrolase activity, using water as the final acceptor, but their physiological role is still unclear (Kaewthai et al., 2013). It is also unclear if xyloglucan can be hydrolyzed by plant endoglucanases from other families. Xyloglucan endoglucanases have been found in seven different glycoside hydrolase families in microorganisms (Attia and Brumer, 2016).

Exoglycosidases also have an important role in xyloglucan metabolism. In Arabidopsis, the α-xylosidase XYL1/AXY3 (Sampedro et al., 2001, 2010; Günl and Pauly, 2011), the α-fucosidase FUC95A/AXY8 (Léonard et al., 2008; Günl et al., 2011), and the β-galactosidase BGAL10 (Sampedro et al., 2012) have been shown to act on xyloglucan. These activities can sequentially remove specific unsubstituted residues from xyloglucan subunits located at the nonreducing end of the polymer, trimming the molecule in the process. Absence of any of them blocks the process and results in significant changes in xyloglucan composition, suggesting that chain trimming by exoglycosidases is normally quite extensive. Mutants in genes encoding these enzymes show growth defects, particularly evident in silique elongation, and additionally, *xyl1* mutants show improved germination under various conditions (Sampedro et al., 2010, 2012; Günl and Pauly, 2011; Sechet et al., 2016). The basis of these phenotypes is not yet understood.

A β-glucosidase activity also is required for complete xyloglucan digestion. One such enzyme was characterized in nasturtium (*Tropaeolum majus*) seedlings, where it plays a role in the mobilization of reserve xyloglucan during germination (Crombie et al., 1998). It is a member of glycoside hydrolase family 3 (Lombard et al., 2014). In this study, we completed the characterization of Arabidopsis xyloglucan exoglycosidases by identifying two Arabidopsis genes from the same family, named *BGLC1* and *BGLC3*, that code for β-glucosidases active against xyloglucan. BGLC1, like previously characterized xyloglucan exoglycosidases, is an apoplastic soluble enzyme. BGLC3, on the other hand, is usually anchored to the plasma membrane. In this location, it could digest specifically loose xyloglucan fragments or oligosaccharides without modifying the xyloglucan chains integrated into the wall structure.

## RESULTS

### Soluble BGLC1 and Membrane-Bound BGLC3 Code for β-Glucosidases Active against Xyloglucan

A β-glucosidase active on xyloglucan was purified previously from nasturtium seedlings (Crombie et al., 1998). A phylogenetic analysis was carried out in order to identify the Arabidopsis genes most closely related to this protein (Fig. 1A; Supplemental Fig. S1). Full-length protein sequences translated from the genomes of *Selaginella moellendorffii*, *Pinus taeda*, *Musa acuminata*, *Ananas comosus*, *Brachypodium distachyon*, *Oryza sativa*, *Vitis vinifera*, *Solanum lycopersicum*, *Populus trichocarpa*, and Arabidopsis were included, as well two previously characterized β-glucosidases from barley (*Hordeum vulgare*), ExoI and ExoII (Hrmova et al., 1996; Varghese et al., 1999). We propose BGLC as the name for the proteins in this clade of family 3 glycoside hydrolases, as BGLU has already been used for family 1 β-glucosidases (Xu et al., 2004).

AtBGLC1 (At5g20950) and AtBGLC2 (At5g20940) appear to be orthologs of the xyloglucan β-glucosidase from nasturtium (TmBGLC1). The next closest homolog is AtBGLC3 (At5g04885), which has a predicted glycosylphosphatidylinositol (GPI) anchor. All the other species analyzed also have one protein each with a predicted GPI anchor (black circles in Fig. 1A), with the exception of *S. moellendorffii*. Although these proteins do not appear as a monophyletic group in the tree, their respective genes all share a phase 2 intron that appears to be surrounded by homologous sequences (Supplemental Fig. S2). This intron is placed just in front of one or two exons that code for the putative GPI anchor and it is not present on other *BGLC* genes.

To check the expression of the three Arabidopsis genes, RT-PCR was performed on rosettes of 14-d-old plants of Columbia and Nossen ecotypes. Expression was detected for *BGLC1* and *BGLC3* but not *BGLC2* (Fig. 1B). After an unsuccessful attempt at heterologous expression of *BGLC1* in yeast, both *BGLC1* and a truncated version of *BGLC3* without its putative GPI anchor

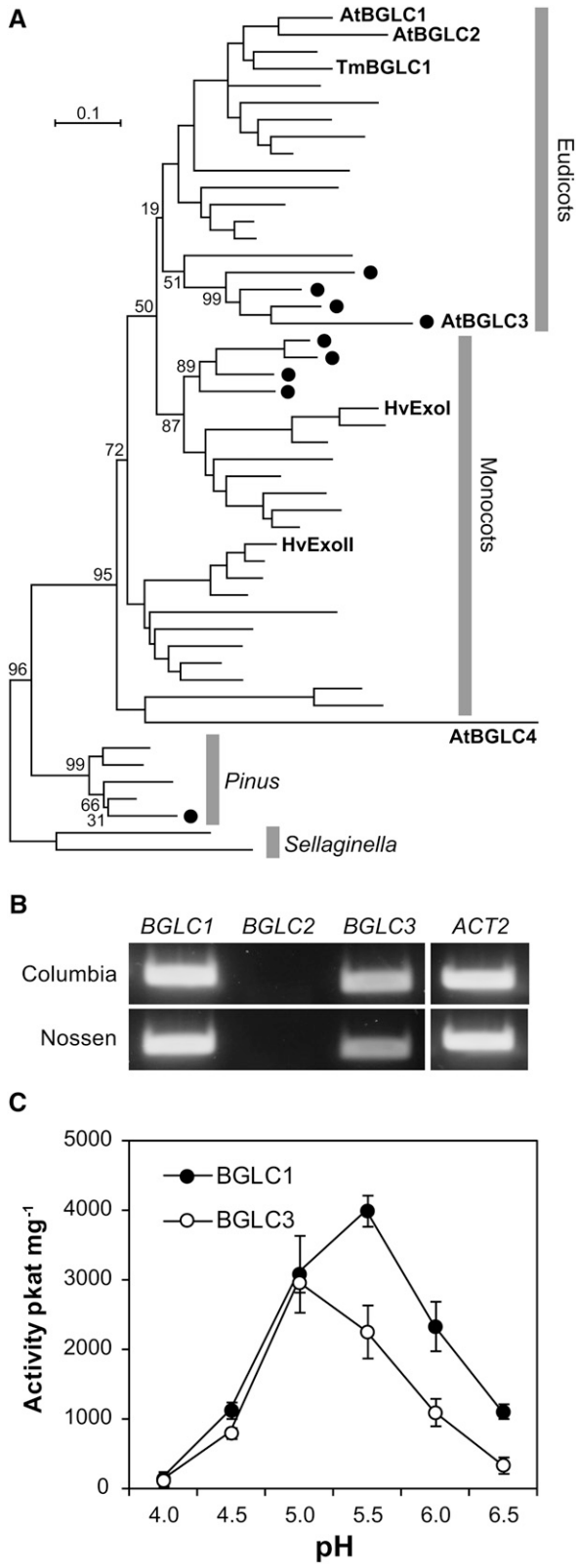


**Figure 1.** Xyloglucan glucosidases in Arabidopsis. A, Phylogenetic tree of close homologs of nasturtium xyloglucan glucosidase from selected species. Nasturtium (TmBGLC1), barley, and Arabidopsis genes are identified. Bootstrap support is shown for selected branches. Black circles identify sequences with a predicted GPI anchor. A detailed tree can be seen in Supplemental Figure S1. B, Transcript levels of glucosidase genes in rosettes from 11-d-old seedlings of Columbia and Nossen ecotypes. The actin gene *ACT2* (*At3g18780*) was used as a control. C, β-Glucosidase activity against GXXG as a function of pH. Extracts were obtained from *N. benthamiana* leaves transiently transformed with overexpression constructs for *BGLC1* (black circles) or *BGLC3* without its GPI signal (white circles). Error bars show SD.

were transiently expressed in *Nicotiana benthamiana* leaves (Fig. 1C). β-Glucosidase activity against xyloglucan was quantified using GXXG obtained by digesting commercial XXXG with AxlA, an α-xylosidase from *Aspergillus niger* (Scott-Craig et al., 2011). Leaves expressing both genes showed much stronger glucosidase activity than leaves transformed with an empty vector, showing that both BGLC1 and BGLC3 can act on xyloglucan. The apparent pH optimum was 5.5 for BGLC1 and 5 for BGLC3.

### Mutants in *BGLC1* Lack Soluble β-Glucosidase Activity against Xyloglucan

Two insertional mutants in *BGLC1* were investigated, *bglc1-1* (Riken 52-0513-1) in ecotype Nossen and *bglc1-2* (SALK_058396) in ecotype Columbia (Fig. 2A). The transposon present in *bglc1-1* is located close to the end of the second intron, while *bglc1-2* appears to be missing the first 28 bp of the last exon. While soluble protein extracts of *bglc1-1* rosettes had no detectable β-glucosidase activity against xyloglucan (Fig. 2B), *bglc1-2* plants showed only a partial reduction in activity and were not studied further (data not shown). Using primers that cover the insertion site, a very low level of properly spliced RNA was detected in *bglc1-1* plants (Fig. 2C).

To determine the function of *BGLC3*, two independent mutants, *bglc3-1* (SAIL _23_E08) and *bglc3-2* (SALK_101370), were studied. Both mutants are in the Columbia ecotype and have T-DNA insertions located in exons (Fig. 2A). Protein extracts from both mutants showed similar activity to those of wild-type plants (Fig. 2B). Although some transcription takes place in both mutants, no properly spliced RNA was detected with primers that cover the respective insertion sites (Fig. 2C).

A prolonged digestion of partially purified XLLG with a *bglc1-1* soluble protein extract resulted in the accumulation of two main oligosaccharides with *m/z* values of 1,247 and 1,115 (Fig. 2D). These most likely correspond to XXLG and GXLG, respectively, since a previous study had shown that Arabidopsis xyloglucan β-galactosidase specifically attacks the Gal closer to the nonreducing end in XLLG (Sampedro et al., 2012). The very low levels of GXXG and XXXG clearly show that β-galactosidase activity is very weak on GXLG, a new result that further clarifies the main pathways of exoglycosidase action on xyloglucan, as revealed by enzyme and mutant analyses (Fig. 3). The

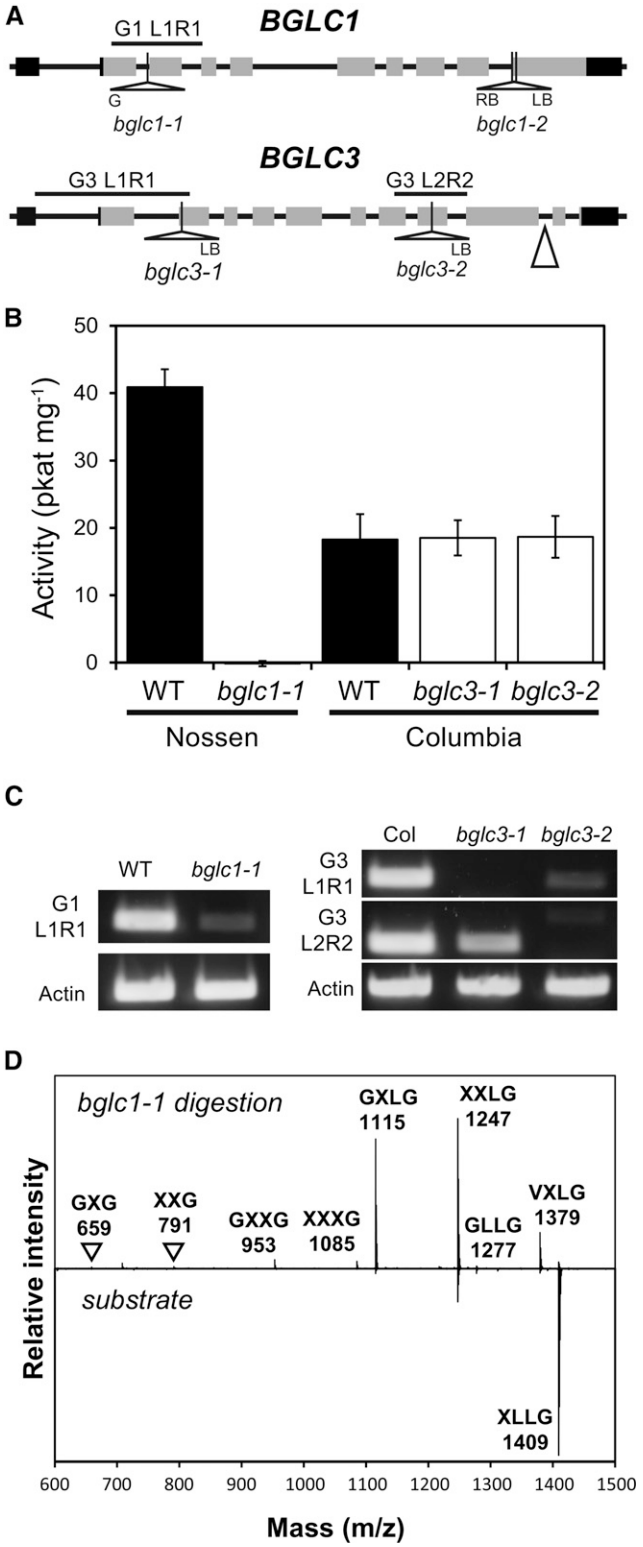


**Figure 2.** Mutants in *BGLC1* and *BGLC3*. A, Models of *BGLC1* and *BGLC3* showing the locations of insertions in the different mutants analyzed. Exons are shown as rectangles, gray in the coding regions and black in the untranslated regions. Black lines above the genes show regions amplified to quantify transcript levels. The triangle shows the localization of a conserved intron in *BGLC* genes coding for GPI-anchored proteins. LB, Left border; RB, right border. B, $\beta$-Glucosidase activity against GXXG in *bglc1* and *bglc3* mutants (white bars) and their corresponding wild types (WT; black bars). Protein extracts were obtained from 14-d-old plants. Error bars show SD. C, Transcript levels of glucosidase genes in *bglc1* and *bglc3* mutants and their corresponding wild types. Primers are identified as in A. The actin gene *ACT2* (*At3g18780*) was used as a control. D, Matrix-assisted laser-desorption ionization time of flight (MALDI-TOF) spectrum of XLLG digested for 24 h with a concentrated *bglc1-1* extract compared with undigested substrate. Ions are identified by their *m/z* and their most likely structure.

extremely low levels of XXG and GXG are consistent with only trace amounts of xyloglucan $\beta$-glucosidase remaining in *bglc1-1* extracts. As for the peak at 1,379 *m/z* units, it has the mass of XXLG plus an additional xylose. It most likely corresponds to a subunit with a side chain of two xylose residues, possibly VXLG, produced by the transxylosidase activity of $\alpha$-xylosidase (Sampedro et al., 2010; Franková and Fry, 2012a, 2012b).

### Partially Digested Xyloglucan Oligosaccharides Accumulate in *bglc1* and *bglc1 bglc3* Mutants But Disappear with Overexpression of Either *BGLC1* or *BGLC3*

Enzyme-accessible xyloglucan from mature leaves of *bglc1-1* plants was compared with xyloglucan from wild-type plants segregated from the mutant line (Supplemental Fig. S3). Mutants showed small amounts of an unusual oligosaccharide with an *m/z* of 1,157, corresponding to the mass of five hexoses, two xyloses, and an acetyl group. This subunit was not detected in wild-type plants. The same ion, obtained from *bglc1-1 bglc3-2* plants, where the intensity was higher, was identified as GXLG after MALDI-TOF/TOF analysis (Fig. 4A). All the expected fragments resulting from single glycosidic cleavages of GXLG were observed. In particular, the intense fragment at 1,025 *m/z* units (loss of xylose) excludes LLG and LLG as the main components of the mother ion. Similarly, the strong *m/z* 701 ion (loss of a xylose and two nonacetylated hexoses at the nonreducing end) excludes GLXG and LLG as well as XLGG or LXGG. Therefore, it seems most likely that GXLG is the main or only component of the 1,157 *m/z* ion in both *bglc1* and *bglc1 bglc3* mutants. It is also reasonable to assume that the ion at 1,115 *m/z* units, which also increases in *bglc1-1*, corresponds to unacetylated GXLG. Together, these ions represent 1.8% of the total xyloglucan fragments detected in *bglc1-1* and less than 0.2% in wild-type plants (Fig. 4B; Supplemental Table S1).

A xyloglucan fragment with an *m/z* of 995, which could correspond to XLG, also accumulated in *bglc1-1*. Other unusual ions that showed increases in *blgc1-1* were those at 791 (from 0.9% to 1.9%) and 953 *m/z* units (from 0.3% to 0.7%). The first corresponds to XXG, and the second could be a mixture of GXXG and XLG. The total sum of these unusual digestion products (XXG, GXXG, XLG, and GXLG), in both acetylated and nonacetylated

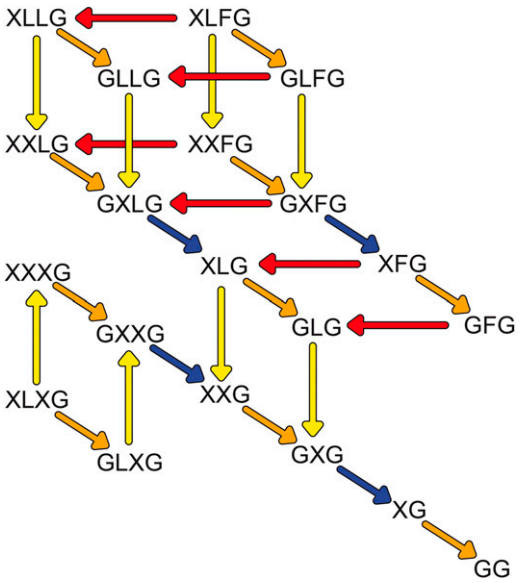


**Figure 3.** Main pathways of xyloglucan degradation by exoglycosidases in Arabidopsis. The activities of the different enzymes are indicated by colored arrows, red for α-fucosidase, orange for α-xylosidase, yellow for β-galactosidase, and blue for β-glucosidase.

forms, was 5.7% of enzyme-accessible xyloglucan in *bglc1-1* and 1.7% in wild-type plants. Among the more common xyloglucan oligosaccharides, an increase in XXLG/XLXG, as well as in XLLG, particularly in their acetylated forms, also was evident, with a corresponding decrease in fucosylated oligosaccharides (Fig. 4B). The accumulation of XLXG or XLXG is not expected in glucosidase-deficient mutants. This was confirmed by MALDI-TOF/TOF analysis of the *m/z* 1,289 ion obtained from *bglc1-1 bglc3-2* plants, which showed a fragmentation pattern corresponding to XXLG (Supplemental Fig. S4).

In contrast with these results, both *bglc3-1* and *bglc3-2* showed no detectable accumulation of unusual oligosaccharides or other significant changes in either enzyme-accessible or enzyme-inaccessible xyloglucan (Supplemental Fig. S5). When enzyme-accessible xyloglucan in a double *bglc1-1 bglc3-1* mutant was compared with segregated wild-type plants from the same cross, the changes in composition were similar but more intense than those observed in *bglc1-1* (Fig. 4C; Supplemental Table S1). In the double mutant, GXLG reached 3.1% of total xyloglucan, compared with 1.9% in *bglc1-1*. The sum of all the unusual digestion products was 7.8% in *bglc1-1 bglc3-1* versus 2.3% in wild-type plants. An increase in XXLG and XLLG also was observed, but only the first was significant. Xyloglucan from *bglc1-1 bglc3-2* plants showed similar changes in composition (Supplemental Fig. S3).

Overexpression constructs for both *BGLC1* and full-length *BGLC3* were used to transform *bglc1-1 bglc3-1*. Both constructs were able to reverse the changes in xyloglucan composition (Fig. 4C). Similar results were observed in two additional lines for each construct. In particular, GXLG was not detected in complementation lines, and the amount of XXLG/XLXG returned to wild-type values. Glucosidase activity was detected in soluble protein extracts in both *35S:BGLC1* and, at much lower levels, in *35S:BGLC3* (Fig. 4D). The activity in these *35S:BGLC3* extracts was not affected by centrifugation at 21,000*g* for 2 h (data not shown), a treatment expected to sediment a majority of microsomes (Abas and Luschnig, 2010). On the other hand, a protein extract enriched in microsomes showed three times higher activity in *35S:BGLC3* than in *35S:BGLC1* (Fig. 4E). This is consistent with BGLC3 being partly anchored to the membrane in these plants. No phenotypic changes were apparent in either single or double mutants, although a subtle change in double mutants would have been difficult to detect, as the phenotype of the plants showed some variation due to the cross between Nossen and Columbia ecotypes.

### Mutations in *BGLC1* and *BGLC3* Have Larger Effects on Xyloglucan Composition in Fucosidase-Deficient Plants

To analyze further the alterations in xyloglucan metabolism caused by glucosidase deficiencies, *bglc1-1 bglc3-1* plants were crossed to *axy8-6*, a mutant deficient in xyloglucan fucosidase (Günl et al., 2011). In the double and triple mutant combinations that were selected from this cross, ions with *m/z* values of 1,261 and 1,303 were observed (Supplemental Fig. S6). These sizes correspond to five hexoses, two xyloses, and a fucose in both unacetylated and acetylated forms. The *m/z* 1,303 ion, obtained from a *bglc1 bglc3 axy8* plant, was identified as GXFG though MALDI-TOF/TOF analysis (Fig. 5A). The spectrum was dominated by the fragment resulting from the loss of fucose as well as the ions resulting from the loss of fucose together with additional residues. The *m/z* 1,025 and 1,171 ions indicate the presence of a terminal xylose, excluding LFG as the dominant component. Similarly, the clear signal at 701 *m/z* units (loss of fucose, a xylose, and two nonacetylated hexoses at the nonreducing end) excludes XFGG or GFXG. Therefore, the 1,261 and 1,303 *m/z* ions observed in these crosses most likely correspond to GXFG and GXFG. In enzyme-accessible xyloglucan, these oligosaccharides were not detected in *axy8* plants but amounted to 4.4% in *axy8 bglc1*, 0.5% in *axy8 bglc3*, and 10% in *axy8 bglc1 bglc3* plants (Fig. 5B; Supplemental Table S2).

Xyloglucan from *axy8* plants released FG, GFG, and XFG fragments that were not present in wild-type plants, as had been described previously (Günl et al., 2011). While FG did not show consistent changes, the proportion of GFG was reduced from 18% in *axy8* to 12% in *axy8 bglc1*, it was unchanged in *axy8 bglc3*, and it was further reduced to 6% in *axy8 bglc1 bglc3* plants. Unacetylated XFG showed similar changes, with a reduction from 1.7% in *axy8* to 1.3% in *axy8 bglc1*, no significant changes in *axy8 bglc3*, and a further reduction

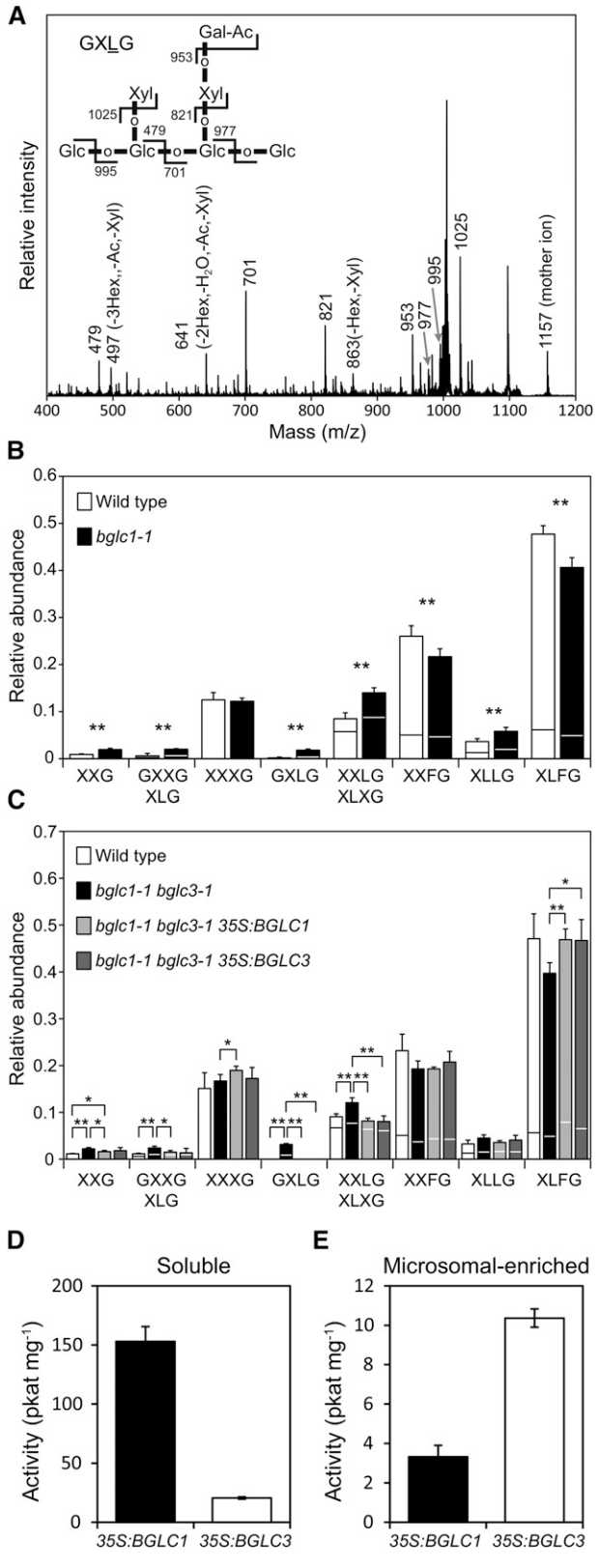


**Figure 4.** Changes in xyloglucan composition in glucosidase mutants and complementation lines. A, MALDI-TOF/TOF spectrum of the 1,157 *m/z* ion from *bglc1-1 bglc3-2* xyloglucan. Fragments produced by single glycosidic cleavages are indicated by their *m/z* in the spectrum and the structure. For selected fragments produced by double cleavages, the losses are indicated in parentheses (Hex for hexose, Xyl for xylose, and Ac for acetyl group). B, Xyloglucan composition in mature leaves from *bglc1-1* (black bars) and wild-type plants (white bars) segregated from the mutant line. Xyloglucan was extracted with endoglucanase from alcohol-insoluble residues of at least three plants, and peak areas were quantified in MALDI-TOF spectra to estimate SD, presented as error bars. The proportion of acetylated subunits corresponds to the area above the horizontal lines. Asterisks indicate significant differences at $P < 0.05$ (*) or $P < 0.01$ (**). C, Xyloglucan composition in *bglc1-1 bglc3-1* mutants (black bars), wild-type plants segregated from the same cross (white bars), and mutants transformed with overexpression constructs for *BGLC1* (light gray bars) or *BGLC3* (dark gray bars). Symbols are as in B. D, Glucosidase activity in soluble protein extracts of double mutants transformed with overexpression constructs for *BGLC1* (black bar) or *BGLC3* (white bar). E, Glucosidase activity in microsome-enriched fractions of double mutants transformed with overexpression constructs for *BGLC1* (black bar) or *BGLC3* (white bar).

to 1% in *axy8 bglc1 bglc3*. On the other hand, acetylated XFG showed the opposite trend, with an increase from 0.1% in *axy8* to 1.9% in *axy8 bglc1*, no change in *axy8 bglc3*, and a further increase to 2.5% in *axy8 bglc1 bglc3* plants. Changes also were observed in XXG (increases in *axy8 bglc1* and *axy8 bglc1 bglc3*) and GXXG/XLG (increases in all mutant combinations). In contrast, there were no increases in GXLG or XXLG, unlike in glucosidase mutants with fucosidase activity.

After endoglucanase treatment, the remaining enzyme-inaccessible xyloglucan was extracted with NaOH and analyzed (Fig. 5B; Supplemental Table S2). Although the compositional changes went in similar directions, their magnitude was much lower in this fraction, which showed reduced levels of unusual oligosaccharides. The amount of GFG, for example, was less than 20% of that observed in the enzyme-accessible fraction for all mutant combinations. Additionally, *bglc1-1 blgc3-2* was crossed to the galactosidase-deficient mutant *bgal10-1* (Sampedro et al., 2012). Enzyme-accessible xyloglucan composition in the triple mutant *bgal10 bglc1 blgc3* was compared with that of the previously analyzed *bgal10* single mutant (Supplemental Fig. S7). No new ions were detected in the triple mutant, but a strong reduction in LG and GLG fragments was apparent, together with an increase in XXG, a similar trend to that observed in the *axy8* crosses.

### *BGLC1* and *BGLC3* Have Overlapping Expression Patterns

For both *BGLC1* and *BGLC3*, approximately 3 kb of promoter sequence upstream from the start codon was cloned and used to drive the expression of the *GUS* gene. *BGLC3* promoter-reporter lines required about 50% more time than *BGLC1* lines to achieve a similar level of staining. In root tips, reporter expression under the control of the *BGLC3* promoter was concentrated in the meristematic zone (Fig. 6B). In contrast, under the control of the *BGLC1* promoter, expression also was high in the root cap and appeared to extend farther back

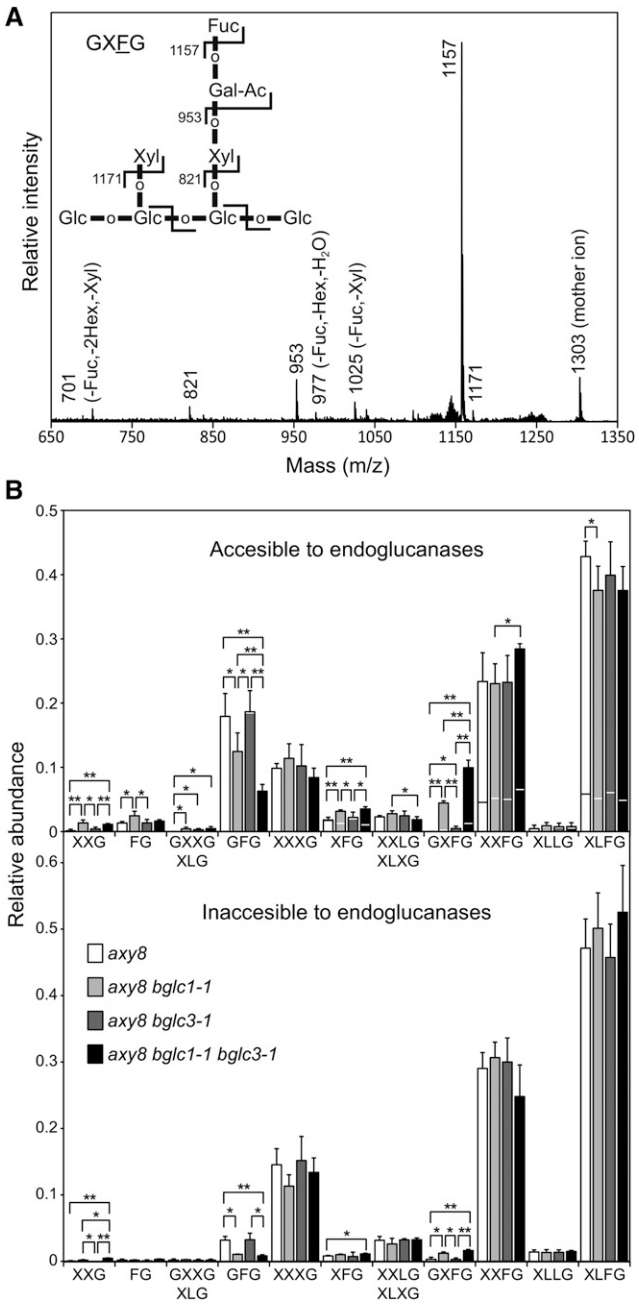


**Figure 5.** Changes in xyloglucan composition in glucosidase mutants deficient in fucosidase activity. A, MALDI-TOF/TOF spectrum of the 1,303 *m/z* ion from *axy8 bglc1-1 bglc3-1* xyloglucan. Fragments produced by single glycosidic cleavages are indicated by their *m/z* in the spectrum and the structure. For selected fragments produced by double cleavages, the losses are indicated in parentheses (Hex for hexose, Xyl for xylose, and Fuc for fucose). B, Xyloglucan composition in mature leaves from *axy8* (white bars), *axy8 bglc1-1* (light gray bars), *axy8 bglc3-1* (dark gray bars), and *axy8 bglc1-1 bglc3-1* plants (black bars). Accessible xyloglucan was extracted with endoglucanase from alcohol-insoluble residues of at least three plants. Inaccessible xyloglucan was then extracted with 17% NaOH. Peak areas were quantified in MALDI-TOF spectra to estimate SD, presented as error bars. The proportion of acetylated subunits corresponds to the area above the horizontal lines. Asterisks indicate significant differences at $P < 0.05$ (*) or $P < 0.01$ (**).

into the elongation zone, particularly in the epidermis (Fig. 6A). Both promoters directed expression to emerging lateral roots as well as the vascular cylinder, where expression became stronger in older parts of the root (Fig. 6, C and D).

In young leaves, reporter expression under the control of the *BGLC1* promoter was stronger in stomata as well as in trichomes and socket cells (Fig. 6, E and G). Diffuse staining also was present in both the lamina and the petiole. In older leaves, expression became stronger in hydathodes and in the vasculature, where it moved to the periphery as the leaf aged. The expression pattern under the control of the *BGLC3* promoter, although similar, showed a number of consistent differences (Fig. 6, F and H). Staining in trichomes was only visible at the earliest stages of development, disappearing much sooner than under the control of the *BGLC1* promoter. At later stages, expression was limited to socket cells (Fig. 6F). Moreover, in both vasculature and hydathodes, strong staining appeared at earlier stages under the control of *BGLC3* than under the control of *BGLC1*.

In the elongating stem, expression was stronger at the tip for both promoters. In flowers, expression also was very similar (Fig. 6, I and J). Staining was present in both sepals and petals, particularly in the vasculature. Reporter expression was particularly strong in anther filaments during elongation as well as in the style, where it started at early stages of development. Strong staining also was observed in abscission zones, starting soon before abscission. Expression also was evident in pedicels. Finally, in developing siliques, staining in the valves was observed during elongation with both promoters (Fig. 6, K and L).

## DISCUSSION

We have identified two Arabidopsis genes in family 3 of glycoside hydrolases, *BGLC1* and *BGLC3*, that code for β-glucosidases capable of removing unsubstituted Glc residues from the nonreducing end of xyloglucan molecules (Fig. 1C). *BGLC1* is most likely an ortholog of the nasturtium β-glucosidase that contributes to xyloglucan digestion during reserve mobilization in seedlings, here named *TmBGLC1* (Crombie et al., 1998). It also could be orthologous to ExoI and ExoII, two β-glucosidases expressed in germinated barley (Hrmova et al., 1996; Varghese et al., 1999). These two enzymes can hydrolyzed both β(1→4) and β(1→3) bonds and have been assumed to act on mixed-linkage glucan during germination.

*BGLC3*, unlike other characterized β-glucosidases, codes for a protein with a predicted GPI anchor. Homologous proteins with predicted GPI anchors also were found in other species analyzed (Fig. 1A; Supplemental Fig. S1). In a proteomic study, BGLC3 was identified as a GPI-anchored protein in a detergent-resistant membrane fraction (Borner et al., 2005). In a separate study, BGLC3 was localized to the plasma membrane based

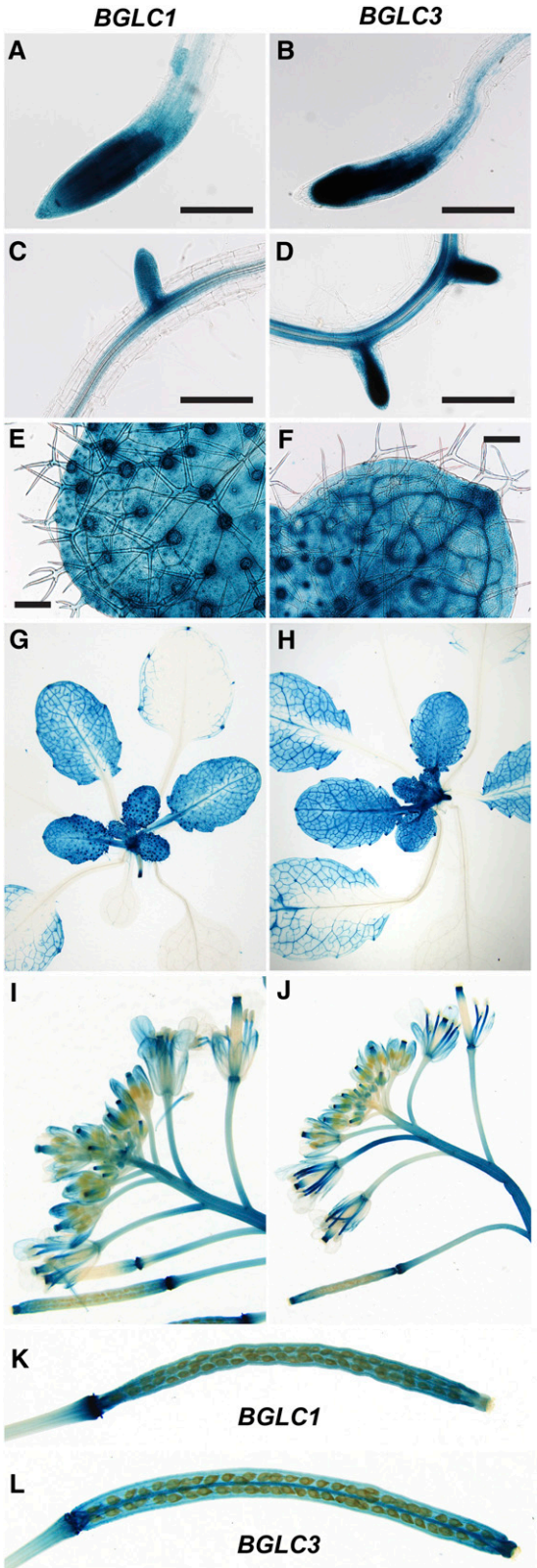


**Figure 6.** Expression of GUS reporter driven by the BGLC1 (A, C, E, G, I, and K) and BGLC3 (B, D, F, H, J, and L) promoters. A and B, Root tips from 14-d-old plants grown on soil. C and D, Roots from 14-d-old plants. E and F, Young leaves from 25-d-old plants. G and H, Rosette leaves from 25-d-old plants. I and J, Flowers at different stages. K and L, Elongating siliques. Bars = 200 $\mu$m.

on its distribution on a density gradient (Dunkley et al., 2006). More recently, BGLC3 has been identified in a membrane fraction enriched in GPI-anchored proteins through phospholipase digestion (Takahashi et al., 2016). That study also analyzed an apoplastic fraction, where it identified BGLC1 but not BGLC3. Microsome-enriched extracts of wild-type plants resulted in activity levels that were too low to be reliably detected (data not shown). However, comparing the activity in *35S:BGLC1* and *35S:BGLC3* plants shows that BGLC3 is concentrated in a microsome-enriched fraction, as would be expected for a protein linked to the plasma membrane (Fig. 4, D and E). Taken together, these results clearly indicate that the identified GPI anchor sequence is functional, at least in Arabidopsis. While in *35S:BGLC3* lines, some of the detected glucosidase activity is soluble, this could be a result of overexpression and might not reflect the situation in wild-type plants.

All the putative GPI-anchored $\beta$-glucosidases share an apparently homologous intron that links the exon or exons coding for the C-terminal signal sequence to the rest of the protein (Supplemental Fig. S2). An homologous intron would imply that the last common ancestor of all these proteins was most likely GPI anchored. The phylogenetic tree indicates that this protein also was the last common ancestor of all the $\beta$-glucosidases in seed plants (Fig. 1A). Considering only branches with higher than 80 bootstrap support, this would mean that soluble proteins evolved at least four times from membrane-anchored ancestors, once in gymnosperms and eudicots and twice in monocots. Support is particularly strong for a separate origin of soluble $\beta$-glucosidases in angiosperms and gymnosperms.

Both *BGLC1* and *BGLC3* RNA, but not *BGLC2*, were detected in young rosettes (Fig. 1B). In a published microarray study of Arabidopsis development, *BGLC1* expression was detected in most samples, while *BGLC2* was expressed only at low levels (39–61 percentile) in some flower samples and at higher levels (75–88 percentile) in developing seeds (Schmid et al., 2005). *BGLC2* expression has also been detected in stomata (Yang et al., 2008) as well as in root procambium and in lateral root cap cells (Brady et al., 2007). It is possible that *BGLC2* plays an analogous role to *BGLC1* in particular tissues. *BGLC3* was not included in Affymetrix microarrays, but the promoter-reporter construct confirms its expression in growing organs with a pattern similar to *BGLC1* (Fig. 6). The other Arabidopsis gene in this clade, *BGLC4*, is highly divergent and has no close homologs in other species. According to a microarray study, it is expressed only in pollen (Schmid et al., 2005).

Both BGLC1 and BGLC3 show activity against xyloglucan oligosaccharides and are most active at the acidic pH found in the apoplast (Fig. 1C). The lower pH optimum for BGLC3 compared with BGLC1 could potentially have physiological consequences, as pH changes are one of the mechanisms that control cell wall expansion (Wolf et al., 2012). The pH optimum of the Arabidopsis enzymes is similar to the 5.25 value observed for the barley β-glucosidases ExoI and ExoII (Hrmova and Fincher, 1997). In contrast, the pH optimum of TmBGLC1, the nasturtium enzyme involved in xyloglucan mobilization in cotyledons, was a bit lower at 4.5 (Crombie et al., 1998). The pH optimum of the Arabidopsis β-glucosidases also was higher than the 4.5 value observed for xyloglucan α-xylosidase in cabbage (*Brassica capitata*; Sampedro et al., 2001). This opens the possibility that small changes in apoplastic pH could modulate the modification of xyloglucan nonreducing ends by favoring xylosidase over glucosidase or vice versa.

### Xyloglucan Changes in Glucosidase-Deficient Plants

Previous studies of xyloglucan exoglycosidase mutants have found an accumulation of partially digested subunits (Sampedro et al., 2010, 2012; Günl et al., 2011; Günl and Pauly, 2011). These subunits are mostly those that cannot be further digested in the absence of the corresponding enzyme, such as XXLG for *xyl1* mutants, GLLG for *bgal10*, or GFG for *axy8* (Fig. 3). These units most likely form at nonreducing ends of xyloglucan chains and then act as acceptors of endotransglycosylation reactions moving to the interior of the chain. Thus, a mutant lacking xyloglucan β-glucosidase activity would be expected to accumulate both GXXG and GXLG subunits, as β-galactosidase does not seem to have much activity against GXLG (Figs. 2D and 3).

Both *bglc1* and *bglc1 bglc3* xyloglucan showed the accumulation of GXLG subunits, most of them acetylated (Fig. 4; Supplemental Table S1). It is also likely that most or all the XLG fragments detected in the glucosidase mutants are the products of endoglucanase digestion of GXLG subunits located within a xyloglucan chain, as was proposed for LG and LLG fragments in *bgal10* mutants (Sampedro et al., 2012). XLG is not expected to accumulate in a glucosidase-deficient mutant with active β-galactosidase. The accumulation of GXXG in these mutants is more difficult to prove, as a small amount of XLG, which has the same size, should be produced by endoglucanase digestion of GXLG subunits. However, in the crosses with fucosidase-deficient plants, no GXLG, XLG, or GXLG is detected; therefore, there is no reason to expect XLG accumulation (Fig. 5B). In these plants, the 953 *m/z* ion, which increases in all glucosidase mutant combinations, should correspond solely to GXXG. The accumulation of GXXG also could explain all or part of the increase in XXG observed, as this fragment could be released from GXXG subunits within xyloglucan chains.

Both *bglc1* and *bglc1 bglc3* show increases in XXLG subunits, particularly in the acetylated form, which doubles in abundance (Fig. 4; Supplemental Table S1). The accumulation of XXLG could be explained by low levels of α-xylosidase or, most likely, the trans-xylosidase activity of this enzyme (Sampedro et al., 2001; Franková and Fry, 2012a, 2012b). In the presence of both XXLG and GXLG, which act as xylose donor and acceptor, respectively, α-xylosidase could maintain an equilibrium between the two forms by moving xylose residues back and forth. This can be seen when XXLG is digested with *bglc1-1* extract (Fig. 2D). The ratio of GXLG to XXLG, together with the acceptor preferences of endotransglycosylases, would determine the ratio of GXLG to XXLG accumulation in xyloglucan chains. The same process could limit the conversion of XXXG into GXXG subunits in glucosidase-deficient plants. It is interesting that, in *bglc1 bglc3* plants, the increase in XXLG and GXLG is of a similar magnitude (Fig. 4C; Supplemental Table S1). In contrast, *axy8* plants accumulate much more GFG than XFG and *bgal10* plants accumulate much more GLLG than XLLG (Günl et al., 2011; Sampedro et al., 2012). This could indicate that GXLG, and possibly also GXXG, are particularly bad acceptors of endotransglycosylation reactions.

Deficiencies in both α-fucosidase and β-glucosidase activities would be expected to produce an accumulation of both GXXG and GXFG subunits in xyloglucan (Fig. 3). This is precisely what was found in *axy8 bglc1*, *axy8 bglc3*, and particularly *axy8 bglc1 bglc3* plants (Fig. 5B; Supplemental Table S2). The accumulation of GXFG takes places mostly in the acetylated form, and this also could account for the accumulation of XFG fragments, as discussed above for XLG. An accumulation of GXLG was not detected, but this is not surprising, as the levels of its precursors XLLG and XXLG appear quite low in *axy8* (Fig. 5B; Supplemental Table S2), particularly if we take into account that the ratio of XXLG to XLXG is lower in fucosidase-deficient plants (Günl et al., 2011). It is somewhat surprising that GXFG and GXFG in *axy8 bglc1 bglc3* accumulate at higher amounts (10%) than GXLG and GXLG in *bglc1 bglc3* plants (3.1%). As these subunits should be formed at similar rates, the most likely explanation is that removal of the fucose renders GXLG a particularly bad acceptor of endotransglycosylation reactions. The levels of GXLG in *bglc1 bglc3* plants are so low that a large part or even all of it could be located at the nonreducing ends of xyloglucan chains.

### The Formation of GFG and Other Three-Glucose Subunits

Xyloglucan from *axy8 bglc1 bglc3* plants contains a considerable proportion of GFG, although it is only one-third of the proportion observed in *axy8* plants (Fig. 5B). This clearly shows that β-glucosidase activity contributes to the formation of these subunits, but it also shows that GFG can be formed when both

β-glucosidases are mutated. In *axy8 bglc1 bglc3*, as in *axy8*, the proportion of GFG is higher in the xyloglucan fraction accessible to enzymes. In addition, all the fucosidase mutants show a similar ratio of accessible GFG to enzyme-inaccessible GFG. This suggests that this subunit is the product of xyloglucan metabolism after deposition in the wall, when a fraction of the polymer has already become inaccessible to enzymes. As leaf xyloglucan appears to be synthesized as a chain of four-glucose subunits, most GFG, even in *axy8 bglc1 bglc3* plants, must result from digestion of a GXFG precursor.

Both *bglc3-1* and *bglc3-2* appear to be null alleles, but some *BGLC1* RNA appears to be present in *bglc1-1* mutants (Fig. 2B). Therefore, it is possible that the formation of GFG from GXFG could be explained by residual activity from BGLC1, followed by α-xylosidase activity (Supplemental Fig. S8). Other members of glycoside hydrolase family 3 also could have activity against xyloglucan, but they are unlikely to play significant roles, at least in growing leaves, as none of them have a predicted GPI anchor and *bglc1-1* has extremely low levels of soluble β-glucosidase activity (Fig. 2, B and D). Alternatively, in the absence of β-glucosidase activity, the formation of GFG could also be explained by an endoglucanase or endotransglycosylase capable of severing xyloglucan chains in front of two unsubstituted Glc residues. The fragment XXXGGXFG could then result in a reducing end XXXGG and a nonreducing end XFG (Supplemental Fig. S8). α-Xylosidase activity could then produce a GFG subunit. Characterization of XTH proteins from both *P. trichocarpa* and nasturtium has shown that they do not require a xylose residue at −2 for activity (Fanutti et al., 1996; Saura-Valls et al., 2008).

Whatever mechanism explains the formation of GFG in *axy8 bglc1 bglc3* also would explain the presence of GLG in *bgal10-1 bglc1-1 bglc3-2* (Supplemental Fig. S7). As for FG in *axy8* and LG in *bgal10* plants, these are most likely fragments of GFG and GLG subunits released by endoglucanase digestion. An interesting observation is that both GFG and GLG always accumulate in unacetylated form, except for a trace amount of GFG detected in *axy8 bglc3* (Supplemental Table S2). XFG is also almost completely unacetylated in *axy8* xyloglucan. In contrast, several partially digested four-glucose subunits accumulate in acetylated form in different exoglycosidase mutants, such as GXLG in *bglc1 bglc3* (Fig. 4B), GXFG in *axy8 bglc1 bglc3* (Fig. 5B), and GLLG in *bgal10* (Supplemental Fig. S7). These subunits form at the nonreducing end of the chain, but the xyloglucan acetylesterase does not seem to be able to completely remove the acetyl group. On the other hand, when an acetylated four-glucose subunit loses the nonreducing Glc to form a three-glucose subunit, the acetyl group is usually removed too. This could be explained by an acetylesterase with strong activity against three-glucose subunits, such as GFG, XFG, or GLG, but much lower activity against four-glucose subunits. As discussed above, acetylated XLG and XFG in glucosidase-deficient mutants are most likely fragments of GXLG and GXFG subunits, respectively.

**The Roles of Xyloglucan β-Glucosidases**

All previously characterized xyloglucan exoglycosidases in Arabidopsis are soluble activities codified by single genes (Iglesias et al., 2006; Sampedro et al., 2010, 2012; Günl and Pauly, 2011; Günl et al., 2011). In contrast, we have found two separate β-glucosidases, one soluble and the other at least partially membrane bound, that are capable of digesting the xyloglucan backbone. We have also shown that they both can affect xyloglucan composition in vivo. The accumulation of partially digested subunits in *bglc1* (Fig. 4B) can be easily explained if BGLC3 is not able to reach the subunits that form at the nonreducing ends of xyloglucan chains incorporated into the wall. The disappearance of these subunits in *35S:BGLC3* lines (Fig. 4C) could then be explained by the partial release to the apoplast of soluble BGLC3 activity in the overexpression lines (Fig. 4D). In wild-type plants, soluble BGLC3 activity is very low or nonexistent (Fig. 2B).

The lack of changes in *bglc3* mutants (Supplemental Fig. S5) and the weak phenotype of *axy8 bglc3* plants (Fig. 5B) suggest that BGLC1 can access most of the xyloglucan that is digested by BGLC3. In particular, if BGLC3 had privileged access to xyloglucan chains during synthesis or deposition, we would expect a stronger effect of mutations in this gene in xyloglucan fractions inaccessible to endoglucanases, where BGLC1 would have less opportunity to act, but this is not the case (Fig. 5B; Supplemental Fig. S5). The effect of *bglc3* mutants in xyloglucan can only be seen clearly when BGLC1 activity is eliminated. Double *bglc1 bglc3* mutants show about twice the percentage of partially digested subunits than *bglc1* plants (Fig. 4, B and C). Strong changes in composition also are seen when comparing *axy8 bglc1* and *axy8 bglc1 bglc3* (Fig. 5B). This suggests that BGLC3 has access to significant amounts of soluble xyloglucan. In the absence of both BGLC1 and BGLC3, this xyloglucan, instead of being digested, would be reincorporated into the wall after the formation of partially digested subunits.

Based on the broad specificity of previously characterized family 3 β-glucosidases, it would not be surprising if BGLC1 and BGLC3 had activity against substrates other than xyloglucan in vivo. It is even possible that, for BGLC3 in particular, xyloglucan metabolism is only a secondary role. On the other hand, the similarity of the expression pattern for both *BGLC1* and *BGLC3* supports the idea that they work in concert (Fig. 6). The expression of both genes also is generally similar to that of previously characterized xyloglucan exoglycosidases, suggesting a coordinated regulation of all these genes (Sampedro et al., 2010, 2012; Günl et al., 2011). By being anchored to the membrane, BGLC3, unlike BGLC1, could digest soluble xyloglucan fragments while preserving the nonreducing ends of xyloglucan chains attached to cellulose or other cell wall components. In consequence, adjustments in the ratio of BGLC1 to BGLC3 could differentially regulate the modification of soluble and wall-bound xyloglucan,

as the lack of a single exoglycosidase is sufficient to block xyloglucan digestion. The phylogenetic tree suggests that a similar arrangement could exist in other plants, as all the species investigated appear to have both soluble and GPI-anchored glucosidases (Fig. 1A; Supplemental Fig. S1). β-Glucosidase might be particularly suited to a regulatory role, as its deficit would generate GXXG and GXLG subunits at the nonreducing end of xyloglucan chains. These subunits appear to be particularly bad acceptors of endotransglycosylation reactions and, thus, would block the rearrangement of xyloglucan chains, also avoiding the large changes in xyloglucan composition observed when other exoglycosidases are missing. This also could be the reason that no morphological phenotype was observed in glucosidase mutants.

In wild-type plants, total activity in microsome-enriched fractions is much lower than in soluble fractions, but this could be related to the extraction and assay protocols and may not accurately reflect the proportions of BGLC3 and BGLC1 activity in vivo. The expression pattern of *BGLC1* and *BGLC3* appears to be quite similar, but nonetheless, some differences can be detected. In leaf vasculature and hydathodes, for example, *BGLC3* expression reaches a peak earlier in development than *BGLC1* (Fig. 6). BGLC1 also is more persistent in trichomes and in the root epidermis. It is possible that, at earlier stages, BGLC3 works to digest the surplus of freshly secreted xyloglucan, while BGLC1 is later required to degrade xyloglucan already integrated into the wall. Additional differences could exist in the regulation of these genes during the diurnal cycle or in response to environmental factors. Some GPI-anchored proteins appear to be released to the apoplast (Takahashi et al., 2016), and this seems to be the case for a fraction of BGLC3 activity in *35S:BGLC3* lines (Fig. 4C). The controlled release of this protein could add another layer of regulation. In addition, the localization of BGLC3 to specific areas of the plasma membrane could create variations in xyloglucan metabolism in different regions of the wall. Finally, BGLC3 could also be present in the endomembrane system, where it might have some role in xyloglucan modification during biosynthesis or during its proposed endocytosis (Baluška et al., 2005). Cellular localization studies would be necessary to address these issues.

It is interesting that two XTH proteins, a transglycosylase and a hydrolase, also have been localized to the plasma membrane, although they do not possess a GPI anchor sequence (Zhu et al., 2012, 2014). As with BGLC3, the function of these enzymes could be the modification of freshly secreted xyloglucan as well as oligosaccharides or longer fragments released by soluble hydrolases after incorporation into the wall (Thompson and Fry, 1997). These results suggest that a role for membrane-anchored proteins needs to be incorporated into our understanding of xyloglucan metabolism. Further research will be necessary to determine how extensive this role is and what are its physiological consequences. The possibility that membrane-anchored proteins play a role in the metabolism of pectins or other noncellulosic polymers should also be explored.

## MATERIALS AND METHODS

### Plant Material and Growth Conditions

The mutant line *bglc1-1* (Riken 52-0513-1) was developed by the plant genome project of the RIKEN Genomic Sciences Center (Ito et al., 2002; Kuromori et al., 2004). Mutants *bglc1-2* (SALK_058396) and *bglc3-2* (SALK_101370) were ordered from the collection of the Salk Institute Genomic Analysis Laboratory (Alonso et al., 2003). Mutant *bglc3-1* (SAIL_23_E08) was obtained from the Syngenta Arabidopsis Insertion Library (Sessions et al., 2002). Mutants *bgal10-1* and *axy8-6* have been described previously (Günl et al., 2011; Sampedro et al., 2012). Double and triple mutants were obtained by crosses. Mutants were compared with Columbia wild-type plants (CS60000) or segregants lacking insertions. Arabidopsis (*Arabidopsis thaliana*) plants were grown in 16-h days at 22°C/18°C light/dark temperature and 60 $\mu$mol $m^{-2}$ $s^{-1}$ light intensity. *Nicotiana benthamiana* plants were grown in 16-h days at 24°C/20°C light/dark temperature.

### Phylogeny

Protein sequences were obtained from BLAST searches at the Phytozome database (https://phytozome.jgi.doe.gov). Phylogenetic analysis was done with MEGA6 (Tamura et al., 2013). Sequences were aligned with ClustalW. After complete deletion of alignment gaps, maximum likelihood analysis was carried out using the model with highest score (Whelan and Goldman model with γ-distribution and invariable sites). The tree was obtained with the subtree-pruning-regrafting level-3 method and a strong branch-swap filter. Bootstrap values were based on 200 replicates. GPI-anchor sequences were identified with PredGPI (Pierleoni et al., 2008).

### RT-PCR

RNA was extracted from 11-d-old seedlings using the Spectrum Plant Total RNA Kit (Sigma-Aldrich). The Transcriptor First Strand cDNA Synthesis Kit (Roche) was employed to obtain cDNA. PCRs were carried out using DNA Polymerase (Biotools) and the primers listed in Supplemental Table S3.

### Plant Transformation

Coding sequences for *BGLC1*, *BGLC1* without the stop codon, *BGLC3*, and truncated *BGLC3* without the sequence coding its putative GPI anchor, as well as promoter sequences for both genes, were amplified with Phusion High Fidelity DNA polymerase (Thermo Fisher) using the primers indicated in Supplemental Table S3. Coding sequences were cloned into pENTR/D-TOPO (Invitrogen), *BGLC1* promoter into pDONR Zeo, and *BGLC3* promoter into pENTR5′-TOPO (Invitrogen). For heterologous expression, *BGLC1* without the stop codon and truncated *BGLC3* genes were introduced into pEAQ-HT-DEST3 and pEAQ-HT-DEST1, respectively (Sainsbury et al., 2009), using LR recombination (Invitrogen). *Agrobacterium tumefaciens* cultures transformed with expression constructs, as well as empty plasmid, were grown overnight, centrifuged for 1 min at 1,000g, washed with infiltration medium (0.5% Glc, 10 mM MES, 10 mM $MgSO_4$, and 100 $\mu$M acetosyringone), and resuspended to a final $OD_{600}$ of 1. Infiltrated *N. benthamiana* leaves were collected after 5 d, and glucosidase activity was determined.

Complementation constructs were obtained by introducing full-length *BGLC1* and *BGLC3* sequences into pK2GW7 (Karimi et al., 2007). A fragment including 35S promoter, gene, and terminator was then extracted from these plasmids using *Sac*I and *Apa*I and introduced into the multicloning site of pSUN (Thomson et al., 2011). After floral dipping, seedlings were selected using sulfadiazine. To obtain promoter:reporter constructs, recombination was carried out between entry clones and destination plasmids pMDC162 (Curtis and Grossniklaus, 2003) for *BGLC1* and pMK7S*NFm14GW for *BGLC3*. Staining patterns were studied as described previously (Sampedro et al., 2012).

### Activity Assays

To obtain soluble protein extracts, approximately 0.5 g of 14-d-old Arabidopsis rosettes or *N. benthamiana* leaves was homogenized in liquid $N_2$. Proteins

were extracted for 45 min at 4°C in 2 mL of 100 mM sodium acetate buffer (pH 5), 1 M NaCl, 1% polyvinylpolypyrrolidone, and 0.1% (v/v) protease inhibitor cocktail for plant cell and tissue extracts (Sigma-Aldrich). After centrifugation at 10,000*g* for 15 min, the supernatant was concentrated using Amicon Ultra 30K (Millipore), filtered through a 0.45-$\mu$m membrane, and washed twice with 3 mL of 20 mM sodium acetate buffer (pH 5). Protease inhibitor cocktail at 0.1% (v/v) was added to the second wash. To obtain a microsome-enriched fraction, homogenized leaves were extracted in 1.5 mL of 50 mM sodium acetate buffer (pH 5), 1% polyvinylpolypyrrolidone, and 0.1% (v/v) protease inhibitor cocktail. After two centrifugations at 1,000*g* for 3 min, the supernatant was concentrated and then washed with 3 mL of 20 mM sodium acetate buffer (pH 5). The concentrated extract (200 $\mu$L) was centrifuged at 500*g* for 1 min, and the supernatant was then centrifuged at 21,000*g* for 2 h. The precipitate was finally resuspended in wash buffer.

Protein concentration was quantified with Coomasie Plus (Thermo Scientific). For each assay, 20 $\mu$L of 4.5 mM XXXG (Megazyme) was predigested for 2 h with 1 $\mu$L of concentrated supernatant from *Pichia pastoris* cultures expressing *AxlA*, an $\alpha$-xylosidase from *Aspergillus niger* that can remove the nonreducing end xylose (Scott-Craig et al., 2011). Under these conditions, more than 95% of the XXXG was converted to GXXG without detectable Glc release. After the addition of 40 $\mu$L of protein extract and overnight incubation, Glc was quantified with the D-Glc HK Assay Kit (Megazyme). To determine the pH optimum, 5 $\mu$L of protein extract was mixed with 35 $\mu$L of 0.1 M phosphate citrate buffer at pH from 4 to 6.5, after it was determined that this pH range did not affect Glc quantification. Activity due to BGLC1 or BGLC3 was estimated by subtracting the activity of leaves transformed with empty plasmid. Extracts of *bglc1-1* also were assayed against 1.5 mM XLLG (TCI).

## Xyloglucan Analysis

Approximately 100 mg of mature leaves from 28-d-old plants was homogenized in liquid nitrogen. The powder was washed with 1 mL of 80% ethanol for 10 min at 50°C, followed by 1 mL of pure ethanol for 10 min at room temperature and 1 mL of acetone for 10 min also at room temperature. Samples were centrifuged at 3,000*g* for 5 min between washes. After drying, the samples were washed once with 1 mL of 100 mM NaCl and twice with water, with centrifugations at 18,000*g* for 3 min between washes. Finally, they were resuspended in 400 $\mu$L of 10 mM pyridine-acetate buffer at pH 4.5, with 0.02% thimerosal and 9 units of endocellulase from *Trichoderma longibranchiatum* (Megazyme). Accessible xyloglucan was extracted in an overnight digestion at 37°C. Inaccessible xyloglucan was obtained by washing undigested material with water and then extracting it for 24 h with 900 $\mu$L of 17% NaOH. After centrifugation, the supernatant was neutralized with 300 $\mu$L of acetic acid. Extracted cell wall material was filtered through a 10K centrifugal filter (VWR), repeatedly washed with 10 mM pyridine-acetate buffer at pH 4.5 with 0.02% thimerosal, and digested overnight with 9 units of endocellulase. Samples were finally dried and resuspended in 20 $\mu$L of 10 mM NaCl. Samples were mixed 1:3 (v/v) with SDHB matrix (9 mg $mL^{-1}$ 2,5-dihydroxybenzoic acid and 1 mg $mL^{-1}$ 2-hydroxy-5-methoxybenzoic acid in 70% acetonitrile), and MALDI-TOF, as well as MALDI-TOF/TOF, spectra were obtained as described previously (Sampedro et al., 2012). Under these conditions, only sodium adduct ions were observed.

## Supplemental Data

The following supplemental materials are available.

**Supplemental Figure S1.** Detailed phylogenetic tree of close homologs of *Tropaeolum majus* xyloglucan glucosidase from selected species.

**Supplemental Figure S2.** Alignment of nucleotide and amino acid sequences surrounding the intron conserved in genes coding for GPI-anchored proteins.

**Supplemental Figure S3.** MALDI-TOF spectra of xyloglucan from Nossen ecotype wild type, *bglc1-1*, and *bglc1-1 bglc3-2*.

**Supplemental Figure S4.** MALDI-TOF/TOF spectrum of the 1,289 *m/z* ion from *bglc1-1 bglc3-2* xyloglucan.

**Supplemental Figure S5.** MALDI-TOF spectra of enzyme-accessible and enzyme-inaccessible xyloglucan from Columbia wild type, *bglc3-1*, and *bglc3-2*.

**Supplemental Figure S6.** MALDI-TOF spectra of xyloglucan extracted from mature leaves of *axy8-6* and *axy8-6 bglc1-1 bglc3-2*.

**Supplemental Figure S7.** Xyloglucan composition in *bgal10-1 bglc1-1 bglc3-2* compared with a previous analysis of *bgal10-1*.

**Supplemental Figure S8.** Possible pathways for the formation of GFG subunits in *axy8 bglc1 bglc3*.

**Supplemental Table S1.** Xyloglucan composition in glucosidase mutants and complementation lines.

**Supplemental Table S2.** Xyloglucan composition in crosses between glucosidase and fucosidase mutants.

**Supplemental Table S3.** Primers used in this work.

## ACKNOWLEDGMENTS

We thank Jonathan D. Walton for providing the *P. pastoris* strain expressing AxlA xylosidase.

Received November 4, 2016; accepted December 9, 2016; published December 12, 2016.

## LITERATURE CITED

**Abas L, Luschnig C** (2010) Maximum yields of microsomal-type membranes from small amounts of plant material without requiring ultracentrifugation. Anal Biochem **401:** 217–227

**Alonso JM, Stepanova AN, Leisse TJ, Kim CJ, Chen H, Shinn P, Stevenson DK, Zimmerman J, Barajas P, Cheuk R, et al** (2003) Genome-wide insertional mutagenesis of *Arabidopsis thaliana*. Science **301:** 653–657

**Attia MA, Brumer H** (2016) Recent structural insights into the enzymology of the ubiquitous plant cell wall glycan xyloglucan. Curr Opin Struct Biol **40:** 43–53

**Baluška F, Liners F, Hlavacka A, Schlicht M, Van Cutsem P, McCurdy DW, Menzel D** (2005) Cell wall pectins and xyloglucans are internalized into dividing root cells and accumulate within cell plates during cytokinesis. Protoplasma **225:** 141–155

**Bootten TJ, Harris PJ, Melton LD, Newman RH** (2004) Solid-state $^{13}$C-NMR spectroscopy shows that the xyloglucans in the primary cell walls of mung bean (Vigna radiata L.) occur in different domains: a new model for xyloglucan-cellulose interactions in the cell wall. J Exp Bot **55:** 571–583

**Borner GHH, Sherrier DJ, Weimar T, Michaelson LV, Hawkins ND, Macaskill A, Napier JA, Beale MH, Lilley KS, Dupree P** (2005) Analysis of detergent-resistant membranes in Arabidopsis: evidence for plasma membrane lipid rafts. Plant Physiol **137:** 104–116

**Brady SM, Orlando DA, Lee JY, Wang JY, Koch J, Dinneny JR, Mace D, Ohler U, Benfey PN** (2007) A high-resolution root spatiotemporal map reveals dominant expression patterns. Science **318:** 801–806

**Crombie HJ, Chengappa S, Hellyer A, Reid JSG** (1998) A xyloglucan oligosaccharide-active, transglycosylating beta-D-glucosidase from the cotyledons of nasturtium (*Tropaeolum majus* L) seedlings: purification, properties and characterization of a cDNA clone. Plant J **15:** 27–38

**Curtis MD, Grossniklaus U** (2003) A Gateway cloning vector set for high-throughput functional analysis of genes in planta. Plant Physiol **133:** 462–469

**Dick-Pérez M, Zhang Y, Hayes J, Salazar A, Zabotina OA, Hong M** (2011) Structure and interactions of plant cell-wall polysaccharides by two- and three-dimensional magic-angle-spinning solid-state NMR. Biochemistry **50:** 989–1000

**Dunkley TPJ, Hester S, Shadforth IP, Runions J, Weimar T, Hanton SL, Griffin JL, Bessant C, Brandizzi F, Hawes C, et al** (2006) Mapping the Arabidopsis organelle proteome. Proc Natl Acad Sci USA **103:** 6518–6523

**Eklöf JM, Brumer H** (2010) The XTH gene family: an update on enzyme structure, function, and phylogeny in xyloglucan remodeling. Plant Physiol **153:** 456–466

**Fanutti C, Gidley MJ, Reid JSG** (1996) Substrate subsite recognition of the xyloglucan endo-transglycosylase or xyloglucan-specific endo-(1→4)-$\beta$-D-glucanase from the cotyledons of germinated nasturtium (*Tropaeolum majus* L.) seeds. Planta **200:** 221–228

**Franková L, Fry SC** (2012a) Trans-α-xylosidase and trans-β-galactosidase activities, widespread in plants, modify and stabilize xyloglucan structures. Plant J **71:** 45–60

**Franková L, Fry SC** (2012b) Trans-α-xylosidase, a widespread enzyme activity in plants, introduces (1→4)-α-D-xylobiose side-chains into xyloglucan structures. Phytochemistry **78:** 29–43

**Fry SC, York WS, Albersheim P, Darvill A, Hayashi T, Joseleau JP, Kato Y, Lorences EP, Maclachlan GA, Mort AJ, et al** (1993) An unambiguous nomenclature for xyloglucan-derived oligosaccharides. Physiol Plant **89:** 1–3

**Günl M, Neumetzler L, Kraemer F, de Souza A, Schultink A, Pena M, York WS, Pauly M** (2011) AXY8 encodes an α-fucosidase, underscoring the importance of apoplastic metabolism on the fine structure of *Arabidopsis* cell wall polysaccharides. Plant Cell **23:** 4025–4040

**Günl M, Pauly M** (2011) AXY3 encodes a α-xylosidase that impacts the structure and accessibility of the hemicellulose xyloglucan in Arabidopsis plant cell walls. Planta **233:** 707–719

**Hayashi T** (1989) Xyloglucans in the primary cell wall. Annu Rev Plant Physiol Plant Mol Biol **40:** 139–168

**Hrmova M, Fincher GB** (1997) Barley beta-D-glucan exohydrolases: substrate specificity and kinetic properties. Carbohydr Res **305:** 209–221

**Hrmova M, Harvey AJ, Wang J, Shirley NJ, Jones GP, Stone BA, Høj PB, Fincher GB** (1996) Barley beta-D-glucan exohydrolases with beta-D-glucosidase activity: purification, characterization, and determination of primary structure from a cDNA clone. J Biol Chem **271:** 5277–5286

**Iglesias N, Abelenda JA, Rodiño M, Sampedro J, Revilla G, Zarra I** (2006) Apoplastic glycosidases active against xyloglucan oligosaccharides of *Arabidopsis thaliana*. Plant Cell Physiol **47:** 55–63

**Ito T, Motohashi R, Kuromori T, Mizukado S, Sakurai T, Kanahara H, Seki M, Shinozaki K** (2002) A new resource of locally transposed Dissociation elements for screening gene-knockout lines in silico on the Arabidopsis genome. Plant Physiol **129:** 1695–1699

**Kaewthai N, Gendre D, Eklöf JM, Ibatullin FM, Ezcurra I, Bhalerao RP, Brumer H** (2013) Group III-A XTH genes of Arabidopsis encode predominant xyloglucan endohydrolases that are dispensable for normal growth. Plant Physiol **161:** 440–454

**Karimi M, Bleys A, Vanderhaeghen R, Hilson P** (2007) Building blocks for plant gene assembly. Plant Physiol **145:** 1183–1191

**Kuromori T, Hirayama T, Kiyosue Y, Takabe H, Mizukado S, Sakurai T, Akiyama K, Kamiya A, Ito T, Shinozaki K** (2004) A collection of 11 800 single-copy Ds transposon insertion lines in Arabidopsis. Plant J **37:** 897–905

**Léonard R, Pabst M, Bondili JS, Chambat G, Veit C, Strasser R, Altmann F** (2008) Identification of an Arabidopsis gene encoding a GH95 alpha1,2-fucosidase active on xyloglucan oligo- and polysaccharides. Phytochemistry **69:** 1983–1988

**Lerouxel O, Choo TS, Séveno M, Usadel B, Faye L, Lerouge P, Pauly M** (2002) Rapid structural phenotyping of plant cell wall mutants by enzymatic oligosaccharide fingerprinting. Plant Physiol **130:** 1754–1763

**Lombard V, Golaconda Ramulu H, Drula E, Coutinho PM, Henrissat B** (2014) The carbohydrate-active enzymes database (CAZy) in 2013. Nucleic Acids Res **42:** D490–D495

**Miedes E, Suslov D, Vandenbussche F, Kenobi K, Ivakov A, Van Der Straeten D, Lorences EP, Mellerowicz EJ, Verbelen JP, Vissenberg K** (2013) Xyloglucan endotransglucosylase/hydrolase (XTH) overexpression affects growth and cell wall mechanics in etiolated Arabidopsis hypocotyls. J Exp Bot **64:** 2481–2497

**Nishitani K, Vissenberg K** (2007) Roles of the XTH protein family in the expanding cell. *In* JP Verbelen, K Vissenberg, eds, The Expanding Cell. Springer-Verlag, Berlin, pp 89–116

**Park YB, Cosgrove DJ** (2012a) Changes in cell wall biomechanical properties in the xyloglucan-deficient *xxt1/xxt2* mutant of Arabidopsis. Plant Physiol **158:** 465–475

**Park YB, Cosgrove DJ** (2012b) A revised architecture of primary cell walls based on biomechanical changes induced by substrate-specific endoglucanases. Plant Physiol **158:** 1933–1943

**Park YB, Cosgrove DJ** (2015) Xyloglucan and its interactions with other components of the growing cell wall. Plant Cell Physiol **56:** 180–194

**Pauly M, Albersheim P, Darvill A, York WS** (1999) Molecular domains of the cellulose/xyloglucan network in the cell walls of higher plants. Plant J **20:** 629–639

**Pauly M, Keegstra K** (2016) Biosynthesis of the plant cell wall matrix polysaccharide xyloglucan. Annu Rev Plant Biol **67:** 235–259

**Peña MJ, Kong Y, York WS, O'Neill MA** (2012) A galacturonic acid-containing xyloglucan is involved in *Arabidopsis* root hair tip growth. Plant Cell **24:** 4511–4524

**Pierleoni A, Martelli PL, Casadio R** (2008) PredGPI: a GPI-anchor predictor. BMC Bioinformatics **9:** 392

**Rui Y, Anderson CT** (2016) Functional analysis of cellulose and xyloglucan in the walls of stomatal guard cells of Arabidopsis. Plant Physiol **170:** 1398–1419

**Sainsbury F, Thuenemann EC, Lomonossoff GP** (2009) pEAQ: versatile expression vectors for easy and quick transient expression of heterologous proteins in plants. Plant Biotechnol J **7:** 682–693

**Sampedro J, Gianzo C, Iglesias N, Guitián E, Revilla G, Zarra I** (2012) AtBGAL10 is the main xyloglucan β-galactosidase in Arabidopsis, and its absence results in unusual xyloglucan subunits and growth defects. Plant Physiol **158:** 1146–1157

**Sampedro J, Pardo B, Gianzo C, Guitián E, Revilla G, Zarra I** (2010) Lack of α-xylosidase activity in Arabidopsis alters xyloglucan composition and results in growth defects. Plant Physiol **154:** 1105–1115

**Sampedro J, Sieiro C, Revilla G, González-Villa T, Zarra I** (2001) Cloning and expression pattern of a gene encoding an alpha-xylosidase active against xyloglucan oligosaccharides from Arabidopsis. Plant Physiol **126:** 910–920

**Saura-Valls M, Fauré R, Brumer H, Teeri TT, Cottaz S, Driguez H, Planas A** (2008) Active-site mapping of a Populus xyloglucan endotransglycosylase with a library of xylogluco-oligosaccharides. J Biol Chem **283:** 21853–21863

**Schmid M, Davison TS, Henz SR, Pape UJ, Demar M, Vingron M, Schölkopf B, Weigel D, Lohmann JU** (2005) A gene expression map of *Arabidopsis thaliana* development. Nat Genet **37:** 501–506

**Schultink A, Liu L, Zhu L, Pauly M** (2014) Structural diversity and function of xyloglucan sidechain substituents. Plants (Basel) **3:** 526–542

**Scott-Craig JS, Borrusch MS, Banerjee G, Harvey CM, Walton JD** (2011) Biochemical and molecular characterization of secreted α-xylosidase from *Aspergillus niger*. J Biol Chem **286:** 42848–42854

**Sechet J, Frey A, Effroy-Cuzzi D, Berger A, Perreau F, Cueff G, Charif D, Rajjou L, Mouille G, North HM, et al** (2016) Xyloglucan metabolism differentially impacts the cell wall characteristics of the endosperm and embryo during Arabidopsis seed germination. Plant Physiol **170:** 1367–1380

**Sessions A, Burke E, Presting G, Aux G, McElver J, Patton D, Dietrich B, Ho P, Bacwaden J, Ko C, et al** (2002) A high-throughput *Arabidopsis* reverse genetics system. Plant Cell **14:** 2985–2994

**Takahashi D, Kawamura Y, Uemura M** (2016) Cold acclimation is accompanied by complex responses of glycosylphosphatidylinositol (GPI)-anchored proteins in Arabidopsis. J Exp Bot **67:** 5203–5215

**Takeda T, Furuta Y, Awano T, Mizuno K, Mitsuishi Y, Hayashi T** (2002) Suppression and acceleration of cell elongation by integration of xyloglucans in pea stem segments. Proc Natl Acad Sci USA **99:** 9055–9060

**Tamura K, Stecher G, Peterson D, Filipski A, Kumar S** (2013) MEGA6: Molecular Evolutionary Genetics Analysis version 6.0. Mol Biol Evol **30:** 2725–2729

**Thompson JE, Fry SC** (1997) Trimming and solubilization of xyloglucan after deposition in the walls of cultured rose cells. J Exp Bot **48:** 297–305

**Thomson JG, Cook M, Guttman M, Smith J, Thilmony R** (2011) Novel sulI binary vectors enable an inexpensive foliar selection method in Arabidopsis. BMC Res Notes **4:** 44

**Tuomivaara ST, Yaoi K, O'Neill MA, York WS** (2015) Generation and structural validation of a library of diverse xyloglucan-derived oligosaccharides, including an update on xyloglucan nomenclature. Carbohydr Res **402:** 56–66

**Vanzin GF, Madson M, Carpita NC, Raikhel NV, Keegstra K, Reiter WD** (2002) The mur2 mutant of *Arabidopsis thaliana* lacks fucosylated xyloglucan because of a lesion in fucosyltransferase AtFUT1. Proc Natl Acad Sci USA **99:** 3340–3345

**Varghese JN, Hrmova M, Fincher GB** (1999) Three-dimensional structure of a barley beta-D-glucan exohydrolase, a family 3 glycosyl hydrolase. Structure **7:** 179–190

**Wolf S, Hématy K, Höfte H** (2012) Growth control and cell wall signaling in plants. Annu Rev Plant Biol **63:** 381–407

**Xiao C, Zhang T, Zheng Y, Cosgrove DJ, Anderson CT** (2016) Xyloglucan deficiency disrupts microtubule stability and cellulose biosynthesis in Arabidopsis, altering cell growth and morphogenesis. Plant Physiol **170:** 234–249

**Xu Z, Escamilla-Treviño L, Zeng L, Lalgondar M, Bevan D, Winkel B, Mohamed A, Cheng CL, Shih MC, Poulton J, et al** (2004) Functional genomic analysis of *Arabidopsis thaliana* glycoside hydrolase family 1. Plant Mol Biol **55:** 343–367

**Yang Y, Costa A, Leonhardt N, Siegel RS, Schroeder JI** (2008) Isolation of a strong Arabidopsis guard cell promoter and its potential as a research tool. Plant Methods **4:** 6

**Zhu XF, Shi YZ, Lei GJ, Fry SC, Zhang BC, Zhou YH, Braam J, Jiang T, Xu XY, Mao CZ, et al** (2012) XTH31, encoding an in vitro XEH/XET-active enzyme, regulates aluminum sensitivity by modulating in vivo XET action, cell wall xyloglucan content, and aluminum binding capacity in *Arabidopsis*. Plant Cell **24:** 4731–4747

**Zhu XF, Wan JX, Sun Y, Shi YZ, Braam J, Li GX, Zheng SJ** (2014) Xyloglucan Endotransglucosylase-Hydrolase17 interacts with Xyloglucan Endotransglucosylase-Hydrolase31 to confer xyloglucan endotransglucosylase action and affect aluminum sensitivity in Arabidopsis. Plant Physiol **165:** 1566–1574